

# Towards intelligent fiber laser design by using a feed-forward neural network

Xinyang Liu<sup>1, \*</sup> and Regina Gumenyuk<sup>1,2</sup>

<sup>1</sup>Laboratory of Photonics, Tampere University, Korkeakoulunkatu 3, Tampere 33720, Finland

<sup>2</sup>Tampere Institute for Advanced Study, Tampere University, Kalevantie 4, Tampere 33100, Finland

## ABSTRACT

We demonstrated a high accuracy prediction of the fiber laser output parameters by using a feed-forward neural network. We explored both the gain and spectral filter parameters to test the prediction performance of the neural network and realized the mapping between cavity parameters and laser output performance. We also investigated how the number of hidden layers could influence the accuracy of prediction. Based on the results, the output spectrum and temporal pulse profiles can be predicted with high accuracy in various fiber laser designs. Our work paves the way to intelligent laser design with ultimate autonomy.

**Keywords:** Intelligent laser cavity design, feed-forward neural network, laser output prediction

## 1. INTRODUCTION

Innovative fiber laser designs enhanced by machine learning algorithms ground the basis for realizing intelligent lasers architecture. The genetic evolutionary algorithm as an optimizer and a neural network as a predictor act together as a powerful tool enabling prediction, self-optimization and self-maintenance functionality of the fiber laser systems [1-3]. Although a fiber laser cavity can be numerically modelled by the generalized nonlinear Schrödinger equation (GNLSE), which incorporates multiple nonlinear and dispersive effects, the converging of a laser cavity is time-consuming using the conventional split-step Fourier method. Considering the output of a laser cavity can be influenced by various intracavity parameters, when it comes to the laser design with the desired output, fast prediction by neural network clearly shows an advantage. In this work, we demonstrate that a feed-forward neural (FNN) network can be used for predicting the output of a fiber laser cavity with high accuracy, including both the spectral and temporal pulse profiles. We also investigate how the number of hidden layers and neurons can influence the prediction accuracy. We explore both the gain and spectral filter parameters to test the prediction performance of the trained FNN model and realize direct mapping from cavity-parameter space to output-parameter space.

## 2. LASER CAVITY SIMULATION AND DATA PRE-PROCESSING

A mode-locking fiber laser cavity with a linear structure is used as the testing platform. The schematic illustration is shown in Fig. 1. A conceptual saturable absorber Mirror (SAM) is employed as a mode-locker. The other end of cavity is terminated by a reflective mirror (M). L1-L4 indicates four pieces of passive fiber, with a length of 25 cm each. 50 cm active fiber is placed between L2 and L3, providing optical gain centered at 1040 nm with a 45 nm gain bandwidth. A Gaussian-shaped spectral filter with a central wavelength of 1040 nm is placed between L1 and L2. An output coupler (OC) is placed between L3 and L4 and couples out 10% of optical power.

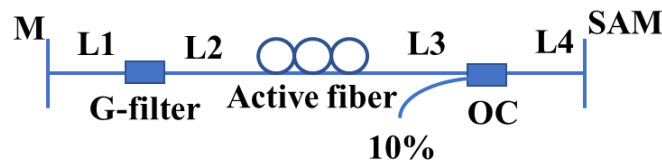


Figure 1. Schematic of the simulated laser cavity in the linear design.

\*xinyang.liu@tuni.fi

The numerical simulation follows laser field propagation within the resonator. The fiber part is simulated by GNLSE:

$$\frac{\partial A}{\partial z} + i \frac{\beta_2}{2} \frac{\partial^2 A}{\partial T^2} = \frac{g}{2} A + i\gamma \left( 1 + i\tau_{\text{shock}} \frac{\partial}{\partial T} \right) \left( A \int_{-\infty}^{\infty} R(t) |A(z, T-t)|^2 dt \right),$$

where  $A(z, T)$  is the complex electrical field,  $z$  is the coordinate of pulse propagation,  $T$  is the retarded time coordinate moving at the group velocity of pulse,  $\beta_2$  is the group velocity dispersion (GVD),  $g$  is the gain coefficient for active fiber,  $\gamma$  is the nonlinear coefficient,  $\tau_{\text{shock}}$  is the shock-formation time-scale that is responsible for the self-steeping effect and  $R(t)$  is the response function that models both the instantaneous electronic (Kerr) nonlinearity and the delayed molecular (Raman) nonlinearity [4]. The GNLSE is solved by the split-step Fourier method using the second order Runge-Kutta algorithm. The saturable gain and SAM are expressed by the model in Ref. [5].

Small signal gain (SSG) and filter bandwidth (FBW) are chosen as variable cavity parameters, respectively, to study prediction capability of FNN for laser output. To prepare the data for training FNN model, SSG is swept from 2 to 22  $\text{m}^{-1}$  with a step of 0.01  $\text{m}^{-1}$ . The FBW is swept from 3 to 13 nm with a step of 0.01 nm. The ranges are chosen to guarantee the laser has enough gain to pulse and is below the threshold for double pulsing.

### 3. FNN PREDICTION

The FNN is trained using MATLAB R2020b. The structure of FNN consists of one input layer, variable hidden layers and one output layer. Since only one cavity parameter is set as an input vector, the input layer only has one neuron. To study the influence of hidden layers and hidden neurons amounts on FNN prediction accuracy, an FNN model with 1-3 hidden layers of 1-5 neurons is trained in a supervised learning manner. The output layer has 161 neurons depending on the number of trimmed data points for the output temporal/spectral intensity profile. Figure 2 shows an example of the structure of FNN with 3 hidden layers of 5 neurons.

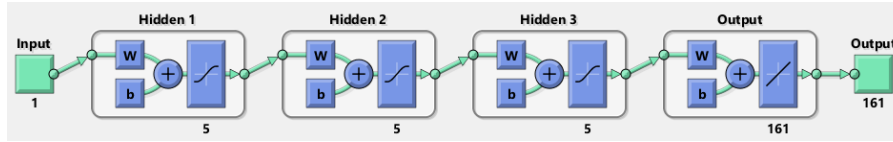


Figure 2. FNN example with 3 hidden layers of 5 neurons.

When the SSG is used as a variable cavity parameter, the training data set is composed of one array of SSG values as an input vector and one array of laser output, i.e., temporal/spectral intensity profiles, as an output vector. The input vector has values from 3 to 21  $\text{m}^{-1}$  with a step of 0.01  $\text{m}^{-1}$ . This excludes SSG values from 2 to 2.99  $\text{m}^{-1}$  and 21.01 to 22  $\text{m}^{-1}$  to use them as training datasets to test the prediction performance of FNN. Once the models are trained, SSG values of 2, 12 and 22  $\text{m}^{-1}$  are used to test the prediction accuracy of the model. The normalized root mean squared error (NRMSE) is used to quantify the prediction error. Figure 3 summarizes the prediction performance of the trained FNN models. When SSG is 12  $\text{m}^{-1}$ , the prediction error is the lowest for both temporal and spectral domains, as this SSG is included in the training dataset. For all three SSGs, NRMSE does not change so much as the layer amount increases. However, the NRMSE decreases as neuron number increases for spectral domain prediction in cases of SSGs equal to 2  $\text{m}^{-1}$  and 12  $\text{m}^{-1}$ . For SSG of 22  $\text{m}^{-1}$ , 2-4 neurons can reduce the NRMSE in the spectral domain. For temporal domain prediction, the NRMSE does not show a clear dependence on the number of hidden layers and hidden neurons. When the SSG value changes, the spectral intensity profile is easily affected by the nonlinearity caused by peak power change; however, temporal domain intensity profile keeps a Gaussian-like single pulse due to limited dispersion. Figure 4 depicts the prediction results with the lowest NRMSE in different cases. The nearly perfect match between GNLSE-generated data and FNN-generated data confirms the FNN can work well to predict fiber laser output.

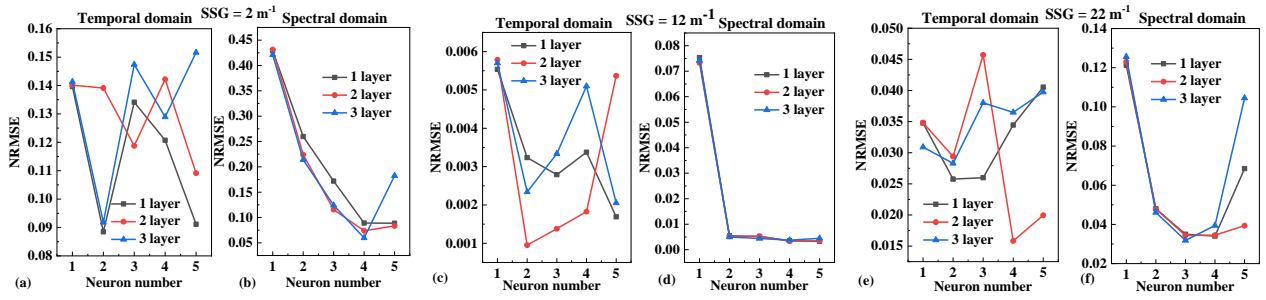


Figure 3. Prediction errors for SSG of  $2 \text{ m}^{-1}$ ,  $12 \text{ m}^{-1}$  and  $22 \text{ m}^{-1}$  in temporal (a,c,e) and spectral domains (b,d,f), respectively.

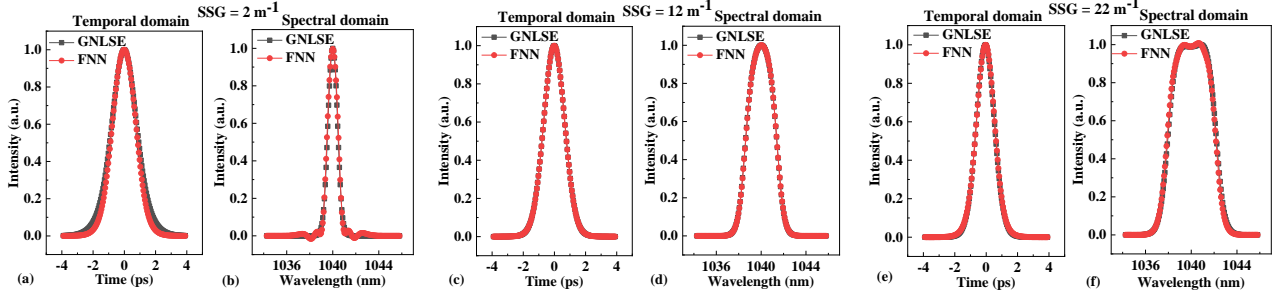


Figure 4. Prediction with the lowest NRMSE for different cases in temporal (a,c,e) and spectral domain (b,d,f). FNN configuration for (a): 1 layer of 2 neurons (NRMSE = 0.088); (b): 3 layers of 4 neurons (NRMSE = 0.060); (c): 2 layers of 2 neurons (NRMSE = 0.00095); (d): 1 layer of 5 neurons (NRMSE = 0.0033); (e): 2 layers of 4 neurons (NRMSE = 0.016); (f): 3 layers of 3 neurons (NRMSE = 0.032).

At the next step, the FBW is set as a variable cavity parameter. The input vector for the training dataset is an array of FBW values, and the output vector for the training dataset is laser output, i.e., temporal/spectral intensity profiles. The input vector varies from 4 to 12 nm with a step of 0.01 nm. The excluded data (3-3.99 nm and 12.01-13 nm) are reserved for testing the prediction accuracy of FNN. Figure 5 summarizes the prediction performance of the trained FNN model. The FNN model gives a relatively accurate prediction when FBW has a value of 8 nm, which is included in the training set. At the same time, the neuron number should be more than one to get the best prediction. When FBW is 3 nm or 13 nm, the prediction accuracy degrades since these two values are outside the training dataset. Figure 6 presents the prediction results with the lowest NRMSE in each case with GNLSE-generated data as a comparison, confirming the prediction ability of the trained model.

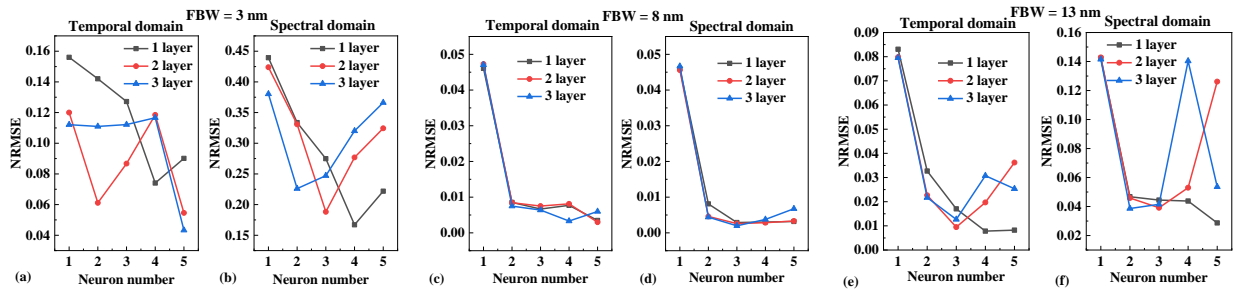


Figure 5. Prediction error for FBW of 3 nm, 8 nm and 13 nm in temporal (a,c,e) and spectral domains (b,d,f), respectively.

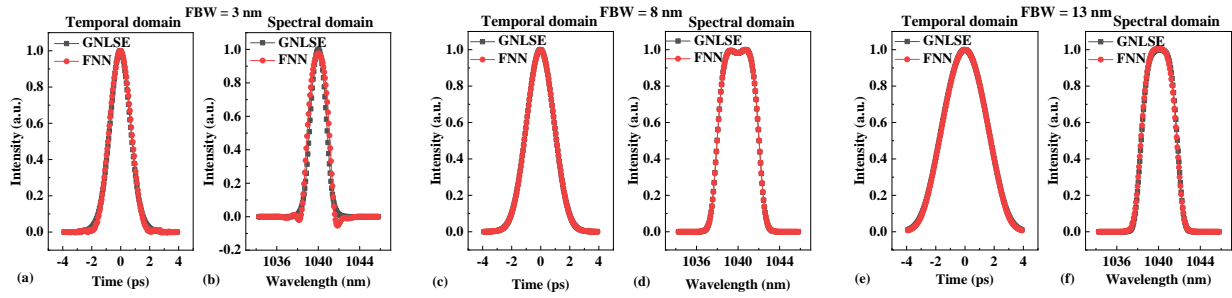


Figure 6. Prediction with the lowest NRMSE for different cases in temporal (a,c,e) and spectral (b,d,f) domain. FNN configuration for (a): 3 layers of 5 neurons (NRMSE = 0.043); (b): 1 layer of 4 neurons (NRMSE = 0.167); (c): 2 layers of 5 neurons (NRMSE = 0.003); (d): 3 layers of 3 neurons (NRMSE = 0.002); (e): 1 layer of 4 neurons (NRMSE = 0.008); (f): 1 layer of 5 neurons (NRMSE = 0.029).

#### 4. CONCLUSION AND OUTLOOK

In this work, we explored the potential of FNN to predict fiber laser output. The results show that the trained FNN model can work as a direct mapping tool for predicting laser output intensity profiles in both temporal and spectral domains. The number of hidden layers does not have a clear influence on prediction accuracy, but the increase in the number of neurons can positively affect the prediction accuracy. The trained FNN model can bypass the tedious iteration of traditional numerical simulation and paves the way for fast, on-demand laser cavity design with the desired or optimum performance.

#### REFERENCES

- [1] Genty, Goëry, Lauri Salmela, John M. Dudley, Daniel Brunner, Alexey Kokhanovskiy, Sergei Kobtsev, and Sergei K. Turitsyn. "Machine learning and applications in ultrafast photonics." *Nature Photonics* 15, no. 2 (2021): 91-101.
- [2] Wu, Xiuqi, Junsong Peng, Sonia Boscolo, Ying Zhang, Christophe Finot, and Heping Zeng. "Intelligent breathing soliton generation in ultrafast fiber lasers." *Laser & Photonics Reviews* 16, no. 2 (2022): 2100191.
- [3] Girardot, J., A. Coillet, M. Nafa, F. Billard, E. Hertz, and Ph Grelu. "On-demand generation of soliton molecules through evolutionary algorithm optimization." *Optics Letters* 47, no. 1 (2022): 134-137.
- [4] Dudley, John M., Goëry Genty, and Stéphane Coen. "Supercontinuum generation in photonic crystal fiber." *Reviews of modern physics* 78, no. 4 (2006): 1135.
- [5] Schreiber, Thomas, Bülend Ortaç, Jens Limpert, and Andreas Tünnermann. "On the study of pulse evolution in ultra-short pulse mode-locked fiber lasers by numerical simulations." *Optics express* 15, no. 13 (2007): 8252-8262.